CO2M: Copernicus Anthropogenic Carbon Dioxide Monitoring	Study on Spectral Sizing for CO_2 Observations: **Final Report**	Version 1.1 Doc ID: SRON-CSS-TN-2020-002 Date: 30-Nov-2020

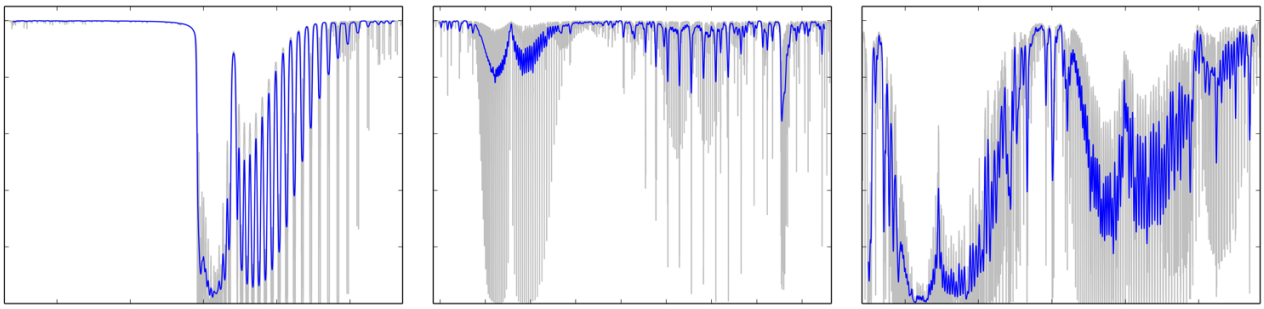

Study on Spectral Sizing for CO_2 Observations: Final Report

Jochen Landgraf, Joost aan de Brugh, Lianghai Wu, Otto Hasekamp, Stephanie Rusli, Hein van Heck
SRON Netherlands Institute for Space Research, Utrecht, The Netherlands

André Butz, Kaspar Graph
Institute of Atmospheric Physics (IPA), Deutsches Zentrum für Luft- und Raumfahrt e.V. (DLR), Oberpfaffenhofen, Germany

Hartmut Boesch
Earth Observation Science Group, University of Leicester, United Kingdom

Leif Vogel
Kaioa Analytics, Bizkaia, Spain

Michael Buchwitz
Institute of Environmental Physics (IUP) / Institute of Remote Sensing (IFE), University of Bremen (UB), Bremen, Germany

Cheng Chen, David Fuertes, Yana Karol and Oleg Dubovik
GRASP SAS, Bachy, France

Study Overview

The atmospheric concentration of the strongest anthropogenic greenhouse gas carbon dioxide (CO_2) increases rapidly due to fossil fuel combustion and changes in land use with serious environmental consequences like global temperature rise, ocean acidification and an increase of extreme weather events. Many nations target a significant reduction of greenhouse gas emissions by the year 2030 (e.g. the EU aims at a 55 % emission reduction), however, at the same time our knowledge about sources and sinks of CO_2 is still limited. Here, satellite observations of the column averaged CO_2 dry air mole fraction (XCO_2) due to anthropogenic point source emissions give both scientists and policy makers a powerful tool at hand to develop and to evaluate mitigation strategy facing future climate change. To derive CO_2 hot spot emissions and the strength of regional CO_2 sources, XCO_2 satellite observations are needed with unprecedented precision and accuracy, good spatial coverage, and high spatial resolution as even the largest CO_2 surface sources produce only small changes in the atmospheric XCO_2.

Currently, the Greenhouse Gases Observing Satellite (GOSAT, Yokota et al., 2009) and the Orbiting Carbon Observatory-2 (OCO-2, Crisp et al., 2017) mission are in orbit, dedicating to observe XCO_2 from space. Additionally, the Carbon Monitoring Satellite (CarbonSat, Bovensmann et al., 2010) was proposed to the European Space Agency (ESA) with the objective to advance our knowledge on the natural and man-made sources and sinks of CO_2 from regional and country up to the local scales, but was not selected for mission implementation. Table 1 lists the spectral and spatial properties of in-orbit and planned satellite instruments observing the Earth reflected sunlight in three spectral bands: the molecular oxygen O_2 A band around 0.765 μm, the weak CO_2 absorption band around 1.61 μm and the strong CO_2 absorption band around 2.06 μm. Concept A and B are derived from the early and the final CarbonSat concept, respectively, where Concept B proposes relatively low spectral resolution and thereby gains signal-to-noise. It was required to keep cost and complexity of the instrument under control and at the same time to meet the demands on spatial coverage. Concepts C, D, and E are adapted from the OCO-2 (Orbiting Carbon Observatory), the MicroCarb concepts and the GOSAT TANSO Fourier transform spectrometer, all featuring relatively high spectral resolution and narrower spectral coverage. Also, the early CarbonSat-A proposal suggested a high-resolution spectrometer concept. This raises the question, which spectral sizing concept of the three-band spectrometer is most appropriate for future CO_2 monitoring from space.

As part of the European Copernicus Programme, the European Commission (EC) and the European Space Agency (ESA) together with the support of the European Organisation for the Exploitation of Meteorological Satellites (EUMETSAT) and the European Centre for Medium-range Weather Forecasts (ECMWF) develops a CO_2 monitoring concept to determine anthropogenic emission of CO_2 as expansion of the Copernicus Space

Component. This asks for a well-balanced design of a satellite payload to be able to address all mission objectives including

- global data coverage
- observation capability of individual CO_2 emission plumes
- high XCO_2 accuracy $\leq$ 0.5 ppm
- high XCO_2 precision $\leq$ 0.7 ppm

with a swath of > 200 km with a coverage requirement of 2-3 days (Meijer et al., 2019, Buchwitz et al, 2020).

This study evaluated the expected level-2 XCO_2 product performance considering realistic signal-to-noise instrument performance and radiometric error sources for a wide range of geophysical scenarios and for various instrument spectral sizing points. It includes errors due to instrument straylight, instrument polarization sensitivity and knowledge errors of the instrument spectral response. Moreover, we amended our analysis with a detailed study of XCO_2 errors caused by erroneous atmospheric light path simulations because of insufficient knowledge on the presence of aerosols and optically thin cirrus. This is complemented by evaluating possible mitigation strategies. Our analysis led to the specification of the spectral sizing of a CO_2 spectrometer covering the O_2 A (760 nm), 1.61 and 2.0 μm band and a concomitant multi-angle polarimeter (MAP) to characterize the atmospheric light path required to meet the mission accuracy requirement.

The study team comprised all European expert groups on CO_2 remote sensing from shortwave infrared measurements using different retrieval algorithms and test data sets to evaluate and ensure a broad consensus on the study conclusions. The study uses the RemoTeC algorithm (SRON, The Netherlands), BESD/C algorithm (IUP Bremen, Germany) and UoL algorithm (University of Leicester, UK), respectively. Here, the XCO_2 retrieval performance is analyzed for simulated measurements with global and regional coverage and for a dedicated test ensemble used in previous CarbonSat analyzes.

Table 1: Instrument spectral coverage of CarbonSat-A and -B, the OCO-2, MicroCarb and GOSAT design

	Spectral ranges (nm)			Resolution(nm)/sampling ratio		
	NIR	SWIR-1	SWIR-2	NIR	SWIR-1	SWIR-2
CarbonSat-A	756-773	1559-1675	2043-2095	0.045/2.5	0.3/2.5	0.13/2.5
CarbonSat-B	747-773	1590-1675	1925-2095	0.1/3.1	0.3/3.1	0.55/3.3
OCO-2	758-772	1591-1621	2042-2081	0.042/2.5	0.076/2.5	0.097/2.5
MicroCarb	758-767	1597-1619	2023-2050	0.032/2.9	0.067/2.9	0.085/2.9
GOSAT	758-775	1560-1720	1920-2080	0.015/1.4	0.08/2.7	0.1/2.7

XCO_2 Precision due to Measurement Noise

Considering the spectral coverage of CabonSat-A, CarbonSat-B, OCO-2, and MicroCarb in Tab. 1, we added realistic estimates of the signal-to-noise performance to design the spectral sizing points A, B, C and D, respectively. For these concepts, we investigated the XCO_2 precision due the spectrometer measurement noise for a global ensemble of about

10 000 geophysical test cases designed to analyze the RemoTeC retrieval performance for realistic aerosol and cirrus loaded scenes for the month January, April, July and October. Figure 1 summarizes our findings on the XCO_2 product noise. For concepts A, B, and C, the XCO_2 precision is typically less than 1 ppm (0.5 ppm) for more than 90% (75%) of the geophysical test cases. Concept D shows significantly larger noise errors with about 75% (50%) of the cases below 1 ppm (0.5 ppm) implying particularly large errors for low sun and dark surfaces i.e. under high-latitude and winter conditions. Moreover, the BESD/C analysis of XCO_2 precision for 15 dedicated CarbonSat test cases supports these finding showing the best XCO_2 noise performance with a mean precision of 0.70 ppm for concept B followed by concept C (0.92 ppm), concept A (0.95), and concept D (1.57).

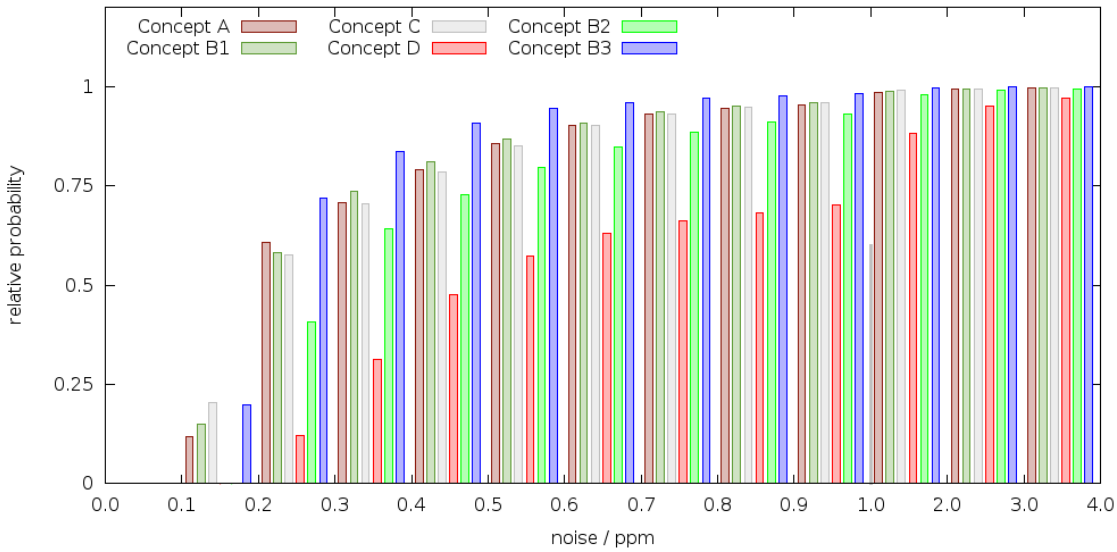

Figure 1: Cumulative histogram of the RemoTeC XCO_2 noise errors for the retrieval concepts A, B1, B2, B3, C, and D. B1, B2, and B3 are retrieval configurations that choose different retrieval windows out of the SW-2 band of concept B (B1=1990-2095nm, B2=2022-2095nm, and B3=1925-2095nm). Please note the change in the x-axis scale at values of 1 ppm.

Instrument Induced Systematic Errors

Next to precision, the XCO_2 product is affected by systematic, instrument induced errors, which are also analyzed for concept A, B, C and D of Tab. 1. Figure 2 summarizes these XCO_2 errors derived with the RemoTeC retrieval software for the global ensemble which was already used in the analysis of Fig. 1. Here we provide the median error of the error distributions of the global data ensemble. A radiometric offset, instrument polarization sensitivity and knowledge errors on the instrument spectral response function (ISRF) shows an error sensitivity which is overall compliant with the mission requirements. The lower spectral resolution of the spectral sizing concept B shows lowest sensitivity to errors in the ISRF. Notable are the relatively larger errors induced by stray light and detector non-linearity, where the latter is characterized by both the mean and the mode (maximum) of the error distribution because of its asymmetric shape with outliers. For both error sources, our instrument description is subject to large uncertainties. It should include

the performance of correction schemes applied in the calibration of flight data, which are hard to estimate in advance of any processor development. Therefore, the overall error contribution should be considered with great care. For this particular reason, our study focused here on the relative differences in error sensitivity for the four instrument concepts rather than on the absolute error contribution. In this perspective, it is striking that the stray light induced XCO_2 error is a factor of two higher for the sizing concept B compared to the other sizing points. When looking at the corresponding stray light induced error contribution per spectral band, we found similar shares for the different spectral sizing concepts. So, the differences in the overall stray light performance was caused by a fortunate error cancelation in the sum of the three band contributions of the high-resolution concepts. We consider this type of error cancelations to be inappropriate to base a trade of between the different sizing concepts.

Overall, the error contributions are reproduced by an independent analysis using the BESD/C algorithm and a limited number of 15 atmospheric cases. Figure 3 indicates the favorable retrieval performance for the low-resolution concept B with larger error contribution for the high-resolution spectral sizing points.

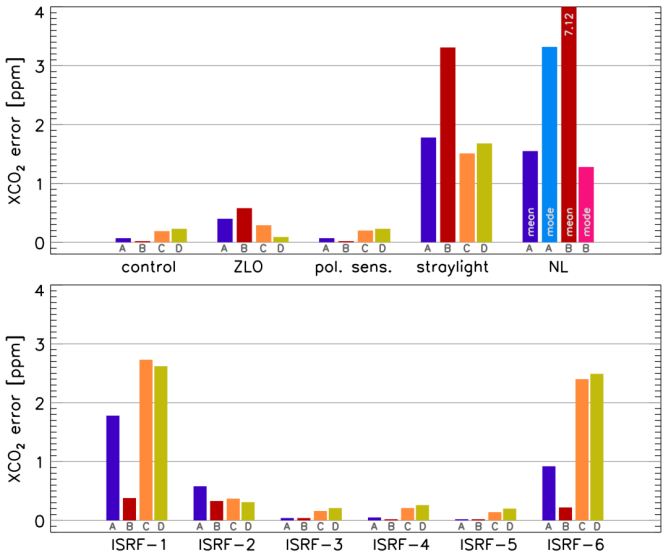

Figure 2: XCO_2 retrieval biases due to instrumental errors for spectral sizing concept A, B, C and D, derived with the RemoTeC retrieval algorithm for global and in case of straylight regional test ensembles. The figure includes the mean bias for the control runs, radiometric offset (ZLO), the polarization sensitivity, spectrometer straylight, detector non-linearity (NL), and six different ISRF distortions. For detector non-linearity, also the mode of the XCO_2 bias distribution is depicted. Here ISRF-1 and -2 describe the effect of a symmetric ISRF distortion, ISRF-3 and -4 that of a corresponding antisymmetric distortion, and ISRF-5 and 6 shows the combined effect of both distortions.

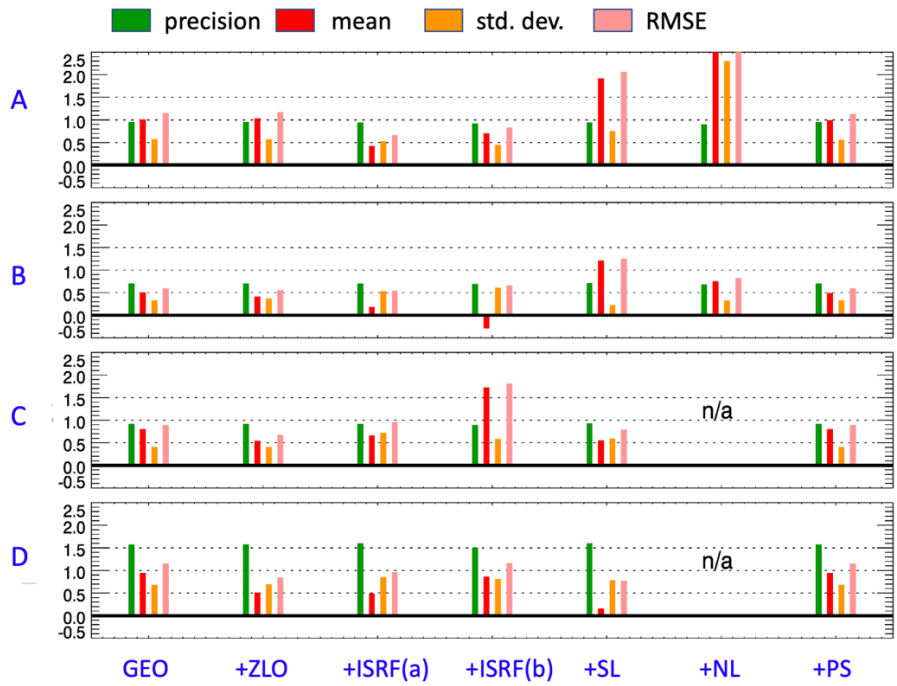

Figure 3: BESD/C error analysis results for 15 atmospheric cases and instruments A, B, C, D (from top to bottom) and different error sources, indicated on the x-axis: geophysical (Geo), i.e., errors due aerosols, clouds, etc., zero level offset (ZLO), Instrument Spectral Response Function (ISRF) anti-symmetrical ("a") and symmetrical ("s") distortions, instrument stray light (stray), detector non-linearity (NL) and instrument polarization sensitivity (PS). The XCO_2 random error ("precision") is shown in green, the three metrics for XCO_2 systematic error are shown in red (from left to right: mean bias, standard deviation of bias, root-mean-square-error).

Aerosol induced errors

To infer XCO_2 from the CO_2 absorption band in the 1.6 μm and 2.0 μm band, the atmospheric light path must be known with high accuracy. After strict cloud filtering, still aerosols and optically thin cirrus may change the light path due to atmospheric scattering. Therefore, to be compliant with the stringent XCO_2 mission requirement, particular attention must be given to scattering induced error in the XCO_2 product. The three-band measurement concepts of the spectral sizing points of our study aims to infer effective aerosol properties from radiance measurement in the O_2 A band at 765 nm and in the strong CO_2 bands at 2.0 μm to describe the atmospheric light path. We investigated the aerosol induced error for the global RemoTeC ensemble. It showed spatial and temporal distribution of aerosol and cirrus induced errors which are driven by the solar zenith angle, the surface albedo, and the amount of cirrus and aerosol content. For all spectral sizing points, we obtained errors < 2 ppm for 50 % (< 4 ppm for 70 %) of the ensemble members, where differences among the concepts are small as indicated in Fig. 4. Therefore, we conclude that aerosol/cirrus induced XCO_2 errors are substantial and the advantages of a high-resolution concept are marginal regarding a better characterization of the atmospheric light path.

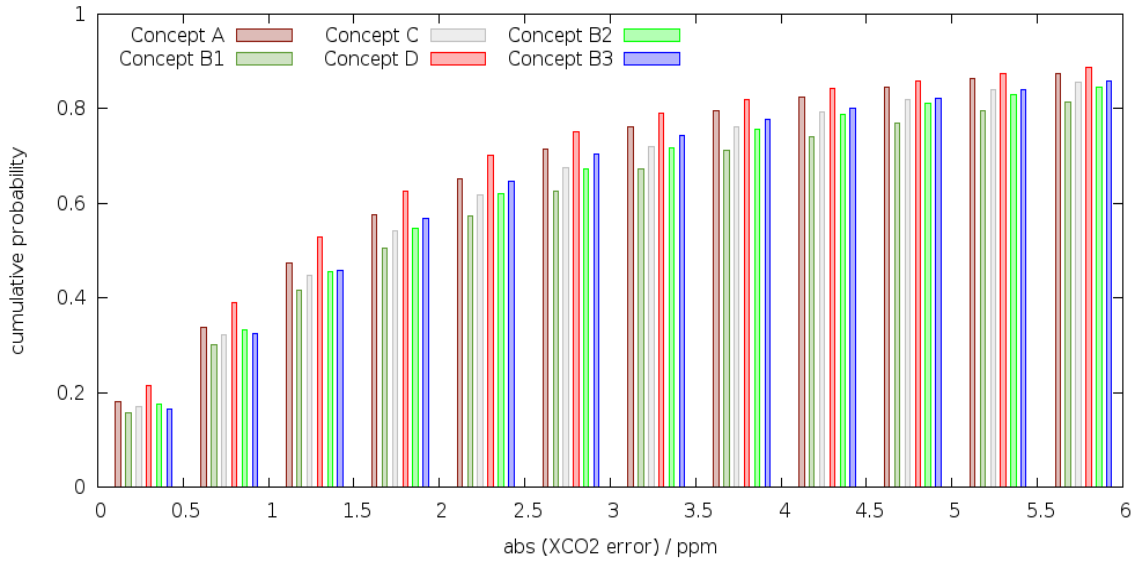

Figure 3: Same as Fig. 1 but for the RemoTeC aerosol and cirrus induced XCO2 error for the retrieval concepts A, B1, B2, B3, C, and D.

Error analysis using GOSAT and OCO-2 observations

To enhance our confidence that the spectral sizing concept B is appropriate for the spectrometer of the CO2M mission, we investigated the impact of spectral resolution on XCO_2 RemoTeC retrieval accuracy using current in-orbit satellite observations. For this purpose, we degraded the spectral resolution of GOSAT and OCO-2 measurements (spectral sizing point C and E in Tab. 1) by convolving the measurements with a spectral smoothing kernel. In this way, real measurements with the spectral resolution of the different spectral sizing points could be generated based on OCO-2 and GOSAT observations. Here, the band width and the signal-to-noise ratio is determined by the OCO-2 and GOSAT instrument and so deviates from the discussed spectral sizing points.

We found that a lower resolution of 0.1, 0.3 and 0.3-0.55 nm in the 0.76, 1.61 and 2.06 µm spectral bands, respectively, mainly induces a larger scatter in the XCO_2 retrieval error, where the scatter gradually increases with lower spectral resolution. Both for GOSAT and OCO-2 measurements, the validation with TCCON XCO_2 ground based measurements showed that the station-to-station variability is largely insensitive to a coarser spectral resolution (Figure 4). For GOSAT, the global XCO_2 bias differs little for the different spectral resolutions. This is not the case for OCO-2 measurements, which show a significant increase in the mean bias for decreasing spectral resolution. Most likely this increase is due to instrument related errors such as a radiance offset in the different bands. Repeating the analysis for corresponding synthetic measurements confirms that single sounding XCO_2 precision decreases for low resolution and the presence of intensity offsets in the different

bands increases biases for lower resolution when not fitted. For CO2M, we expect less scatter in the XCO_2 biases due to the better signal-to-noise performance of the spectrometer.

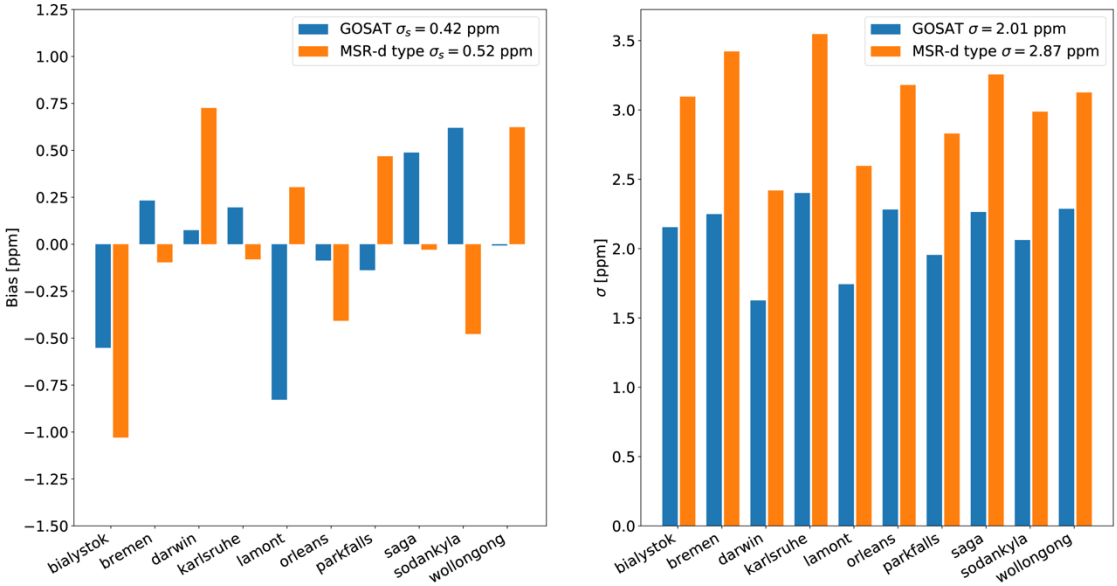

Figure 4. Bias and standard deviation (σ) at different TCCON stations for GOSAT and spectrally degraded GOSAT observations (with a resolution of 0.1nm, 0.3, 0.55 nm in the NIR, SWIR-1 and SWIR-2 spectral band, MSR-d type retrieval). Mean biases of −2.28 and 0.31 ppm are subtracted accordingly for GOSAT and MSR-d type retrievals to show the bias variation on the same reference level.

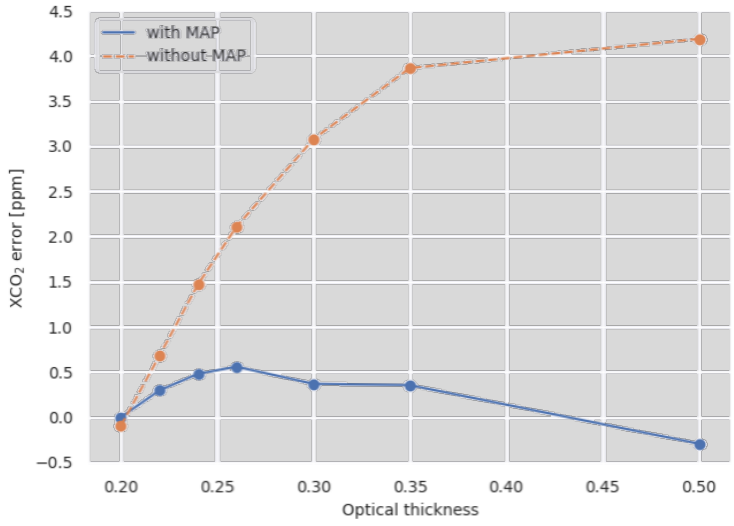

Figure 5: Aerosol induced XCO_2 bias as a function of aerosol optical thickness using only spectrometer measurements of concept B (without MAP) and using spectrometer and MAP observations in a synergistic manner. Simulations are performed for an elevated aerosol layer over a vegetation surface. Simulations are performed with RemoTeC.

The Need of a Multi-Angle Polarimeter

The scattering induced XCO_2 error is one of the main error contributions for a three-band spectrometer concept, as reported in the literature and also confirmed by our study. Thus, to meet the strict XCO_2 accuracy requirement with a satisfying mission data yield, the atmospheric light path must be described more accurately. In the context of our study, we have investigated the benefit of a multi-angle polarimeter (MAP) as an additional payload of the CO2M mission. This measurement concept is well known for aerosol remote sensing as the combination of radiance and polarization measurements in multi-viewing directions shows high sensitivity to aerosol and cirrus scattering properties. Therefore, we analyzed performance requirements of the MAP instrument with respect to the XCO_2 performance. The analysis accounts for two different instrument concepts using the spectral modulation technique and bandpass polarimetry.

For the modulation concept covering the spectral range 385-765 nm with at least five viewing angles, we conclude that the radiance uncertainty must be < 3 % and the degree of linear polarization (DLP) uncertainty must be < 0.0035. The same radiometric requirements hold for the band pass concept, where we assume measurements of radiance and DLP with at least 40 different viewing angles at wavelengths 410, 440, 490, 550, 670, 863 nm. Here, the radiance uncertainty must be also < 3 % and the DLP uncertainty < 0.0035. For instrument cross calibration, it is desirable to have one nadir radiance measurement at 753 nm.

Independent on the MAP concept, the radiance and polarization measurements must the spatially resampled, both for a consistent interpretation of the different viewing angles and for a co-alignment with the CO_2 measurements. For this purpose, a spatial oversampling of a factor 2 in each spatial dimension is required. The benefit of the MAP instrument in light of the XCO_2 accuracy is illustrated in Fig. 5, which shows the XCO_2 accuracy as a function of the aerosol optical thickness for a spectrometer only retrieval and for the synergistic use of a three-band spectrometer and a MAP. Whereas for the spectrometer only retrieval the XCO_2 biases strongly increases for aerosol optical thickness > 0.25, the combined use of the MAP and the spectrometer keeps the error within the requirement.

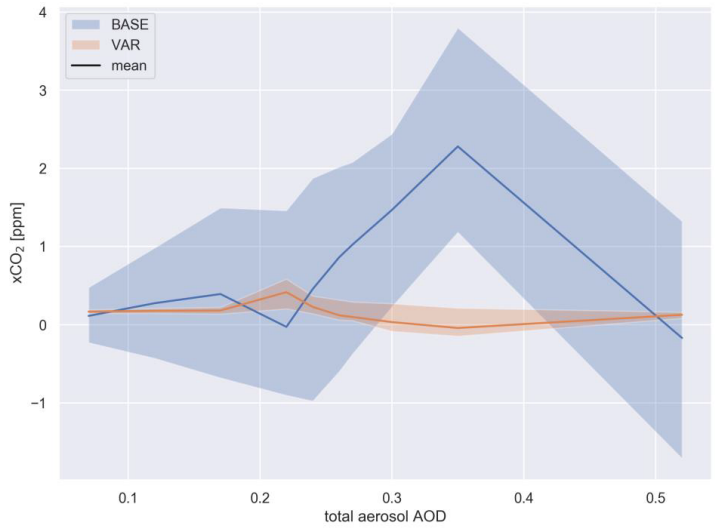

Figure 6: Aerosol induced error as a function of aerosol optical depth AOD for an ensemble of geophysical simulations covering different aerosol scenarios, surface types and geometries using the UoL retrieval approach. Here blue indicates errors for a spectrometer-only retrieval, red the corresponding errors for a synergistic use of spectrometer and MAP observations. The shaded areas show the respective 25%-75% percentile range, whereas the solid line depicts the mean of all biases.

The significant improvement of the XCO_2 performance for a combined spectrometer-MAP data processing was confirmed by an independent analysis tool. We assessed the performance of the UoL retrieval algorithm using prior aerosol information with an accuracy and precision provided by the envisaged MAP aerosol sounder. To this end, the UoL retrieval method was adjusted to use external aerosol information as provided by the polarimeter. Figure 6 depicts the results for a series of geophysical simulations covering different aerosol scenarios, surface types and geometries. Here, 'BASE' indicates the data performance employing no a-priori aerosol information in the retrievals (spectrometer-only performance), where 'VAR' represents the expected XCO_2 accuracy and scatter when using MAP aerosol information as priori aerosol input to the UoL retrieval algorithm. From the figures, it is obvious that the BASE retrieval leads to non-compliant results for the gross of scenarios and aerosol loads. Considering a MAP aerosol product with reduced uncertainties, the VAR retrievals, yields XCO_2 biases which meet the 0.5 ppm XCO_2 threshold values with significant lesser spread in the data. These results clearly highlight the improvements in performance of the UoL retrieval when employing aerosol information from a MAP instrument.

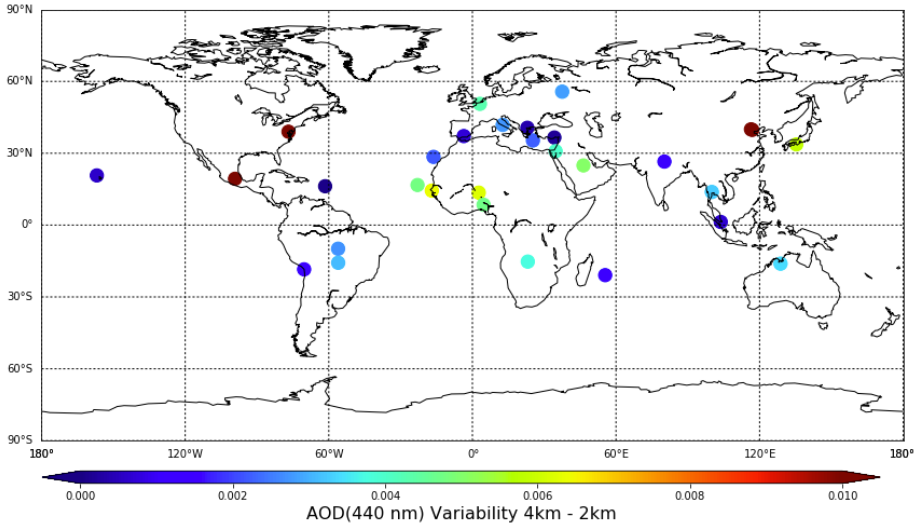

Figure 7: Difference in the mean aerosol optical depth (AOD) for a 2 and 4 km spatial mean obtained for 30 AERONET sites.

The MAP Spatial Resolution

Based on the results and analysis conducted in our study, a MAP enhances significantly the quality of the CO2M XCO_2 data product. Here, it is essential that the MAP observations are resampled to be concentric around the barycentre of a spectrometer spatial sampling. This resampling is performed in a dedicated level-1B to level-1C data processing and requires a spatial oversampling of at least 2 in both spatial directions to minimizing spatial interpolation errors to an acceptable level. To specify the required spatial resolution, we investigated the spatial variability of tropospheric aerosols on the spatial scale of the CO_2 spectrometer sampling of 2×2 km^2. For this purpose, we evaluated the temporal variability of aerosol properties at 30 AERONET ground sites, which was transformed into a spatial variability using the local wind speed. Overall, we found that the spatial variability of tropospheric aerosols is negligible on the scale of CO2M samplings. Specifically, the mean aerosol parameters obtained for a 2 and 4 km spatial scale showed very small differences: only 0.004 for aerosol optical depth (AOD at 440 nm), 0.004 for Angstrom exponent, and 0.004 for aerosol single scattering albedo (see Fig. 7). Such small differences cannot be reliably detected even using the fundamentally most reliable AERONET observations. Moreover, even for extreme events, the aerosol type did not vary on these scales. In contrast, the analysis of maximum spatial variation of aerosol concentrations, some nonnegligible spikes up to 0.2 for AOD (440nm) were observed at spatial scale of 4 km. However, those high fluctuation corresponds to very high aerosol loading event, and remains at ~ 5 to 6% relative level in respect of total AOD. In such situations, decreasing observational resolution to 2 km is unlikely to resolve the problem. Light scattered at different angles is affected by aerosols over neighbouring pixels and the resulting inconsistency is notably higher at smaller spatial scales and quickly decreases with increase of spatial resolution. Thus, the performed study suggests that using 4 km spatial resolution for MAP sensor planned to be deployed as part of CO2M Copernicus mission instead of 2 km is sufficient to capture the features in aerosol variability. Moreover, the observations at 4 km scale are expected to provide significantly more consistent multi-angular information than at 2 km spatial scale.

Conclusions

Based on our extended sensitivity analysis, using both simulated measurements and real measurements of the OCO-2 and GOSAT mission, we draw the following conclusions for the payload of the CO2M Copernicus mission:

1. A three-band spectrometer with the spectral sizing

Band	Spectral range [nm]	Spectral resolution [nm]	Spectral oversampling ratio
NIR	747-773	0.1	3.1
SWIR-1	1590-1675	0.3	3.1
SWIR-2	1925-2095	0.55	3.3

   is appropriate and higher resolution concepts do not provide a significant advantage with respet to this choice. Here, it is desirable to measure the SWIR-2 with a resolution of 0.3 for a reduced band width of 1990-2095 nm as the shorter wavelength in the range 1925-1990 nm provide no extra information assuming a cloud imager with a 1.38 μm band for cirrus detection as an additional payload instrument.
2. For the three-band spectrometer concepts, aerosol induced XCO_2 errors are significant and the performance is non-compliant for all investigated spectral sizing point.
3. A multi-angle polarimeter (MAP) improves the error performance to the required level of accuracy and enhances the data yield of the mission.
4. For a compliant MAP, two different, equally appropriate concepts are investigated:
   - a modulation concept measuring radiance and degree of linear polarization continuously in the spectral range 385-765 nm in at least five different viewing angles
   - a band-pass filter concept, which measures at 6 dedicated wavelength the radiance and DLP in 40 different viewing directions.
5. For both MAP concepts, the radiance and DLP should be measured with an uncertainty of 3 % and 0.0035, respectively.
6. The MAP observations must be resampled around the barycenter of the spatial samples of the CO_2 spectrometer with a resolution ≤ 4 km with an oversampling ratio of at least 2 in both spatial dimensions.

Technical Notes of this study

TN-1	Specification of Instrument Spectral Sizing Concepts, Spectral Errors and Geo-Physical Scenarios
TN-2	Instrument related error for the different spectral sizing of a CO_2 instrument
TN-3	CO_2 errors due to measurement noise and atmospheric scattering for the different spectral sizing concepts of a CO_2 instrument

TN-4	Optimizing Spectral Sizing Concepts
TN-5	Error analysis for CarbonSat scenarios and different spectral sizing
TN-6	Preliminary Recommendations
TN-7	XCO2 retrieval uncertainty under different spectral sizing concepts
TN-8	Requirement study for the Multi-Angle-Polarimeter
TN-9	Aerosol induced XCO2 errors: A literature review
TN-10	Adopting External Aerosol Data in the UoL Retrieval Algorithm and Intercomparison to RemoTeC
TN-11	Aerosol Variability Analysis

Study results published in peer-reviewed journals

Wu, L., aan de Brugh, J., Meijer, Y., Sierk, B., Hasekamp, O., Butz, A., and Landgraf, J.: XCO2 observations using satellite measurements with moderate spectral resolution: investigation using GOSAT and OCO-2 measurements, Atmos. Meas. Tech., 13, 713–729, https://doi.org/10.5194/amt-13-713-2020, 2020.

Rusli, S. P., Hasekamp, O., aan de Brugh, J., Fu, G., Meijer, Y., and Landgraf, J.: Anthropogenic CO2 monitoring satellite mission: the need for multi-angle polarimetric observations, Atmos. Meas. Tech. Discuss., https://doi.org/10.5194/amt-2020-152, in review, 2020.

References

Bovensmann, H., Buchwitz, M., Burrows, J. P., Reuter, M., Krings, T., Gerilowski, K., Schneising, O., Heymann, J., Tretner, A., and Erzinger, J.: A remote sensing technique for global monitoring of power plant CO2 emissions from space and related applications, Atmos. Meas. Tech., 3, 781–811, https://doi.org/10.5194/amt-3-781-2010, 2010.

Meijer Y., et al., Copernicus CO_2 Monitoring Mission Requirements Document, issue 2.0, ESA-ESTEC, EOP-SM/3088/YM-ym, 2019

T. Yokota, T., Yoshida, Y, Eguchi, N., Ota, Y., Tanaka, T., Watanabe, H., Maksyutov S., Global Concentrations of CO_2 and CH_4 Retrieved from GOSAT: First Preliminary Results, SOLA, 2009, Vol. 5, 160–163, doi:10.2151/sola.2009–041

Crisp, D., Pollock, H. R., Rosenberg, R., Chapsky, L., Lee, R. A. M., Oyafuso, F. A., Frankenberg, C., O'Dell, C. W., Bruegge, C. J., Doran, G. B., Eldering, A., Fisher, B. M., Fu, D., Gunson, M. R., Mandrake, L., Osterman, G. B., Schwandner, F. M., Sun, K., Taylor, T. E., Wennberg, P. O., and Wunch, D.: The on-orbit performance of the Orbiting Carbon Observatory-2 (OCO-2) instrument and its radiometrically calibrated products, Atmos. Meas. Tech., 10, 59–81, https://doi.org/10.5194/amt-10-59-2017, 2017.

Buchwitz, M., S. Noël, M. Reuter, J. Landgraf, H. Boesch, H., van Heck, P. Veefkind, Johan de Haan, H. Bovensmann, A. Richter: Final Report ESA Study on Consolidating Requirements and Error Budget for CO_2 Monitoring Mission (CO2M-REB), technical report, in preparation